Available online at www.CivileJournal.org

Civil Engineering Journal

Vol. 6, No. 4, April, 2020

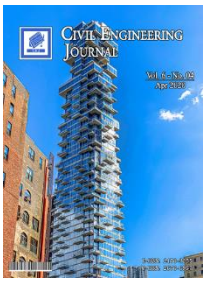

Experimental Study of Large-scale RC Beams Shear-Strengthened with Basalt FRP Sheets

Ahmed M. Sayed [a, b*]

[a] Department of Civil Engineering, College of Engineering, Assiut University, Assiut 71511, Egypt.

[b] Department of Civil and Environmental Engineering, College of Engineering, Majmaah University, Al-Majmaah 11952, Saudi Arabia.

Received 26 December 2019; Accepted 05 March 2020

Abstract

Over the last three decades, many experimental studies have been conducted to investigate the behavior of Reinforced Concrete (RC) beams, shear strengthened with externally bonded Fiber-Reinforced Polymer (FRP) composite. However, the majority of experimental studies have focused on small- to medium-scale beam specimens. As a result, most design equations that have been developed as part of these studies may thus not be accurate at predicting the shear strength of large-scale RC beams shear-strengthened with FRP sheets. This study thus involved performing tests on six specimens to study the effect of the larger scale, along with new variables such as beam width, new varieties of FRP sheets (basalt FRP (BFRP)), and the strengthening configuration (U-jacketing), on the prediction of the ultimate load of RC beams strengthened with externally bonded FRP composite. The experimental results were analyzed and showed that all these variables affected the lateral strain along the bottom and the top of the beams. It was found that variations in the depth to width ratio of the beams caused the failure angle to vary as well. For beams strengthened with BFRP sheets, both the cracking and ultimate load increased to 1.19 and 1.94 times the cracking and ultimate load of the control beams under identical conditions.

Keywords: Large-scale RC Beams; BFRP Sheets; Shear Strengthened; Beam Width; Lateral Strain.

1. Introduction

The technique of applying various types of Fiber-Reinforced Polymer (FRP) sheets to strengthen concrete structures has become a well-recognized method, particularly for strengthening Reinforced Concrete (RC) beams. This is clearly shown by the development of design codes associated with the technique [1]. This technique is used to strengthen RC beams in the shear zone. However, studying the shear behavior of these RC beams is complicated because the mechanisms are complex making the prediction of the shear strength and behavior of these beams difficult. For this reason, in the last three decades, many experimental and numerical studies have been conducted on RC beams strengthened with externally bonded FRP sheets to provide data through which design equations and models can be developed that can predict shear force as accurately as possible [1-3].

Some previous research has taken into account the effect of debonding between the concrete surface and the FRP in suggesting models [4-6]. Several models have also been proposed based on an analytical study carried out on many experimental and numerical tests to provide a database through which to verify the accuracy of the models [7-9]. Because the RC beams in the resistance to shear are complex, therefore many researchers have focused on studying the behavior of RC beams in the shear zone [10-12]. Also from the useful and new properties of basalt BFRP, many

* Corresponding author: a.sayed@mu.edu.sa

http://dx.doi.org/10.28991/cej-2020-03091507

researches have focused on the use of this type of FRP in the strengthening operations, whether in the shear zone [13-15] or in the flexural zone [16-18] or both together [19] with different forms of BFRP, whether sheets or bars [20, 21]. However, these experimental and numerical studies have not considered all the parameters that influence the shear behavior of RC beams strengthening with FRP sheets; such as the beam width, the effect of scale (large-scale dimensions), new types of FRP sheets (such as basalt FRP (BFRP)), and the applied strengthening configuration (U-jacketing). Therefore, using these models to predict shear behavior sometimes does not yield accurate values. The reason for the inaccuracy is that these design equations and models have been proposed based on a limited number of experimental test results on small-scale RC beams. Additionally, they have neglected some of the variables mentioned above.

In previous studies by Sayed et al. (2014) [22] and Deniaud and Cheng (2001) [23], a database of experimental results from more than 300 RC beams was collecting from 40 experimental studies using different types of strengthening configurations. However, in this database, it was observed that the tests were performed only on small-scale RC beams with a total depth and width of less than 500mm and 300mm, respectively. In addition, not many tests took the actual lengths of the RC beam span into account, as is necessary for bridge girders. Additionally, the effect of the actual dimensions of the RC beams on the prediction of shear behavior was rarely taken into account [24-27]. As a result, none of the existing analytical models and design equations directly considers the effect of scale on the calculation of the shear strengthening with externally bonded BFRP composite. Therefore, the shear behaviour of large-scale RC beams strengthened in the shear zone with BFRP sheets will be investigated in this study. Many parameters will be included in the experimental study, such as the effect of larger scales, beam width, type of FRP sheets (BFRP), and strengthening configuration (U-jacketing), in order to provide more realistic data that can be used to predict the shear behavior with higher accuracy.

2. Materials and Methods

2.1. Specimen Details

Six rectangular RC beams were tested. They were simply supported and were of a large scale, with a total height of 1000 mm and beam width varying from 300 to 500 mm with a shear span to depth ratio *a/d* of 1.90, as shown in Figure 1. The beams, under equal two-point static loads 800 mm apart placed symmetrically about the mid-span, were tested up to the point of failure. The concrete standard cubic compressive strength f_{cu} for each beam is shown in Table 1. It was found that these strengths ranged from 48.75 to 49.88 MPa. Two types of steel bars were used to reinforce the RC beams. These were namely deformed steel bars, which were used for longitudinal reinforcement, and plain steel bars, which were used for web vertical reinforcement. Four bar sizes; 10, 16, 25, and 32 mm diameter bars, were used to obtain the same main reinforcement ratio of 3.0% of the concrete cross-sectional area for all beams. The web rebars consisted of 8.0 mm diameter stirrups with yield and ultimate strengths of 430 and 590 MPa, respectively, at a spacing of 200 mm at the shear span zone, and 150 mm at the flexural span, as shown in Figure 1. The main reinforcement yield and ultimate strengths were 488 and 674MPa, respectively, while Young's modulus was 206 GPa.

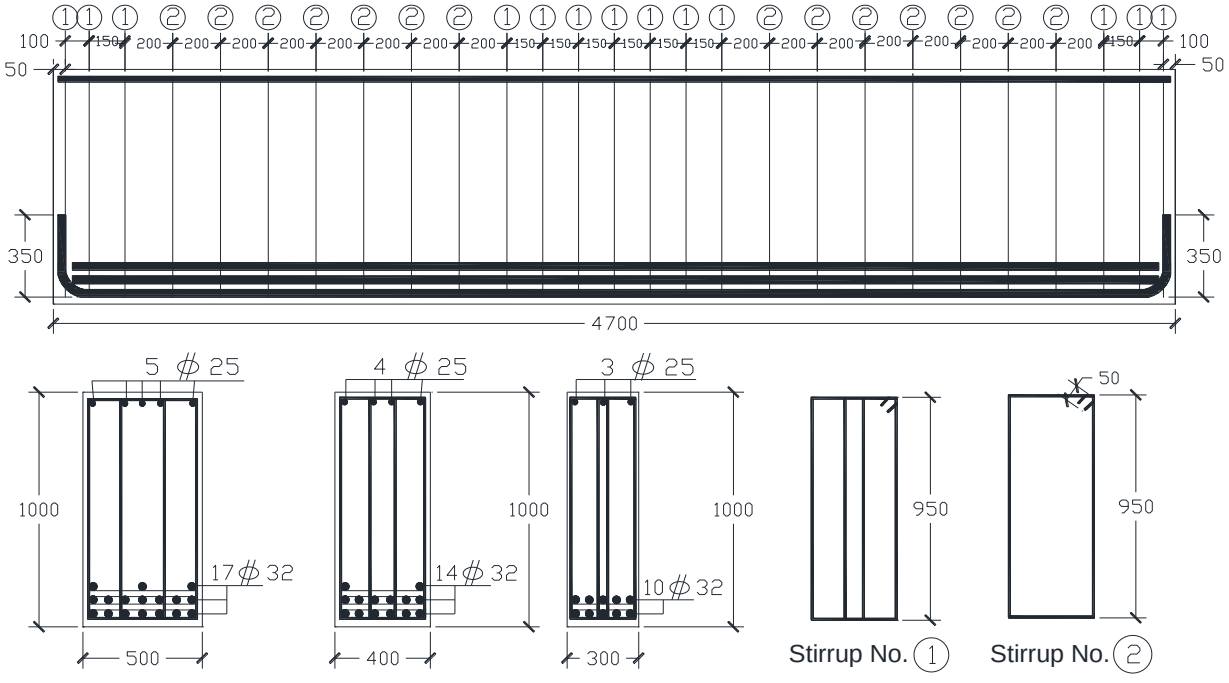

Figure 1. Geometrical details of the large-scale RC beams (all dimensions in mm)

Table 1. Summary of details for the beam specimens analyzed in the present study

Beam specimen	Geometric data				Concrete	Area of steel reinforcement		External shear reinforcement				
	b (mm)	*h* (mm)	*d* (mm)	*a* (mm)	f_{cu} (MPa)	Bottom (mm^2)	Top (mm^2)	$n \times t_f$ (mm)	h_f (mm)	f_{fu} (MPa)	E_f (GPa)	Type
C-1000/300	300	1000	915	1750	48.75	8042	1472	0	0	0	0	0
C-1000/400	400	1000	915	1750	48.75	11259	1963	0	0	0	0	0
C-1000/500	500	1000	915	1750	49.88	13672	2454	0	0	0	0	0
U-B-1000/300	300	1000	915	1750	48.75	8042	1472	4 × 0.157	1000	2100	100	BFRP
U-B-1000/400	400	1000	915	1750	48.75	11259	1963	4 × 0.157	1000	2100	100	BFRP
U-B-1000/500	500	1000	915	1750	49.88	13672	2454	4 × 0.157	1000	2100	100	BFRP

Three specimens that were not strengthened (C-1000/300, C-1000/400, and C-1000/500) were used as control beams to compare with the three beams that were strengthened with continuous BFRP sheets applied at the shear span, as shown in Figure 2. These beams were strengthened with four layers of BFRP sheet as the U-jacketing vertical fiber which possessed a tensile strength, ultimate tensile strain, and an elastic modulus of 2100MPa, 2.1%, and 100GPa, respectively. The bond at the BFRP and concrete interface was made with epoxy adhesive material which possessed an elastic modulus and tensile strength of 3.43 and 51.9 MPa, respectively. A curvature of at least 20mm had to be provided at the cross-sectional corners of the beam when beam strengthening with externally bonded U-jacket BFRP laminate.

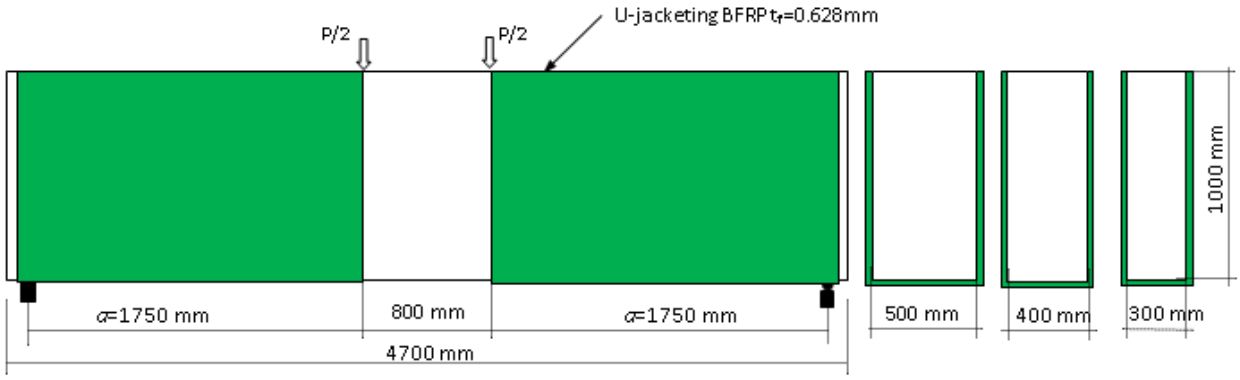

Figure 2. Geometrical details of the RC beams strengthened by U-jacketing with BFRP sheets

2.2. Instrumentation and Test Setup

All beams were tested using a loading machine with a 10000kN capacity to apply monotonic loads at two symmetrically positioned load points. A computer-aided data acquisition system was used to monitor the load, strains, and displacements throughout the loading tests at selected time intervals. The load was applied until the failure load was reached. The typical measurements taken were: vertical deflection of the beam at mid-span, the horizontal displacement of the beam at shear span (out-of-plane), the strain on the BFRP sheets, and the strain on the concrete at the top surface of the beam at mid-span.

To measure the concrete and BFRP sheet strains, electrical resistance strain gauges were attached to the concrete and BFRP sheet surfaces. The deflection at the beam mid-span was measured using linear variable displacement transducers (LVDTs). The main components of the testing equipment included the LVDTs, the strain gauges, the hydraulic jack equipment, and the frame used for testing the control and strengthened beams as shown in Figures 3 and 4. For all specimens, including both control and strengthened beams, five LVDTs were installed on both faces of the beam set 25 mm apart along the diagonal strut to record out-of-plane displacement, as shown in Figure 5.

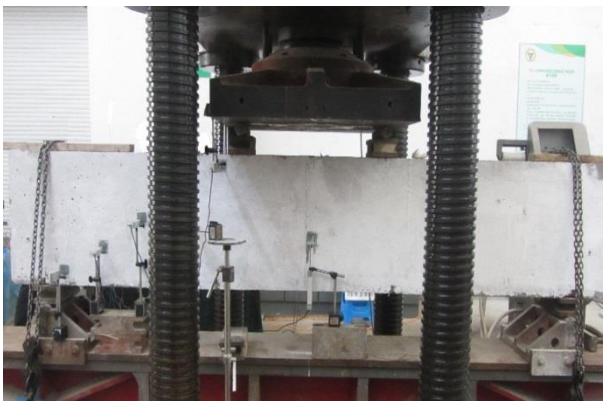

Figure 3. Details of the test setup for a control beam

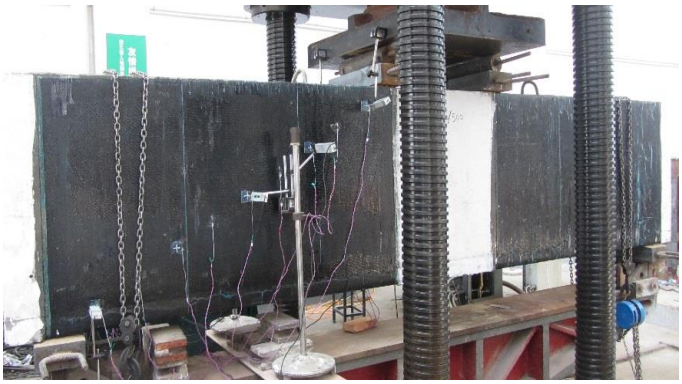

Figure 4. Typical installation of strain gauges and details of the test setup for strengthened beams

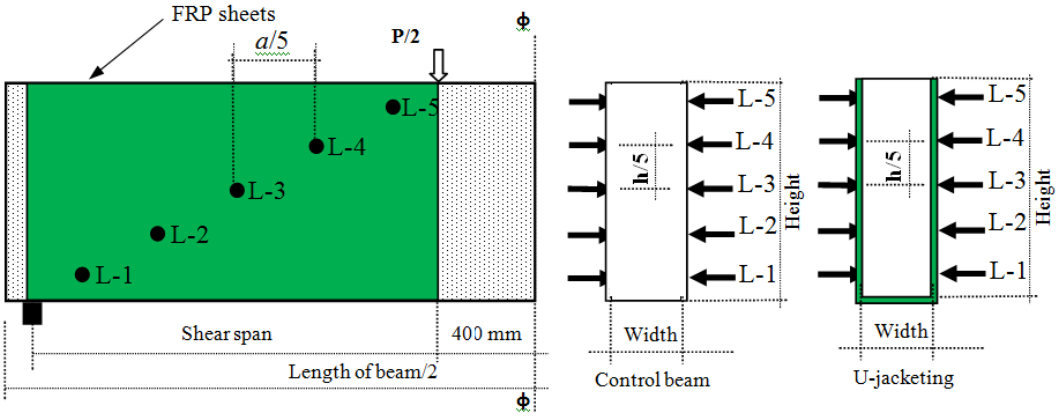

Figure 5. Typical LVDT arrangement for measuring beam out-of-plane displacement

3. Experimental Test Results and Discussion

The results presented were expressed in terms of cracking and ultimate load capacities, mid-span load, deflection, concrete compression strain relationships, out-of-plane displacement, load-BFRP strain relationships, and failure modes. Detailed analysis and discussion of the results will be presented in this section.

3.1. Pattern of Cracks, Shear Capacity and Modes of Failure

The pattern of cracks, shear capacity, and modes of failure was analyzed for all beams in the various beam series as follows:

3.1.1. Large-scale Beam Series (1000/300)

The first crack in the large-scale control beam C-1000/300 was observed at the bottom concrete surface at the mid-span of the beam while it was exposed to a cracking load of 300 kN. By increasing the applied load, the crack increased and the first crack formed at the shear zone at a cracking load equal of 360 kN. The final failure mode was

observed to be a shear-type with an inclination of 43° to the horizontal axis, as shown in Figure 6. The beam test specimen failed at a corresponding applied load of 1260 kN.

The first crack in beam U-B-1000/300 strengthened with four layers of BFRP sheet U-jacketing, started at the bottom concrete surface in the flexural zone under a load application point at a cracking load of 360 kN and propagated vertically up to two-thirds of the height of the beam, as shown in Figure 7. The ultimate load of U-B-1000/300 was 2440 kN, 1.94 times greater than that of the control beam C-1000/300. The mode of failure was noted to be tensile rupture failure of the BFRP sheet, as shown in Figure 7.

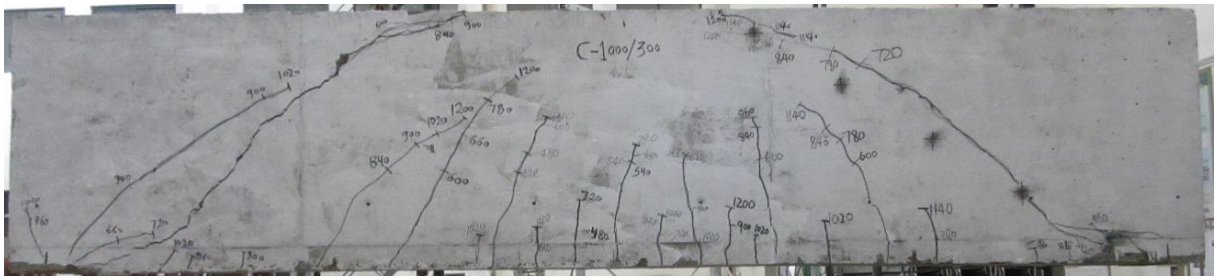

Figure 6. Control beam crack pattern (C-1000/300)

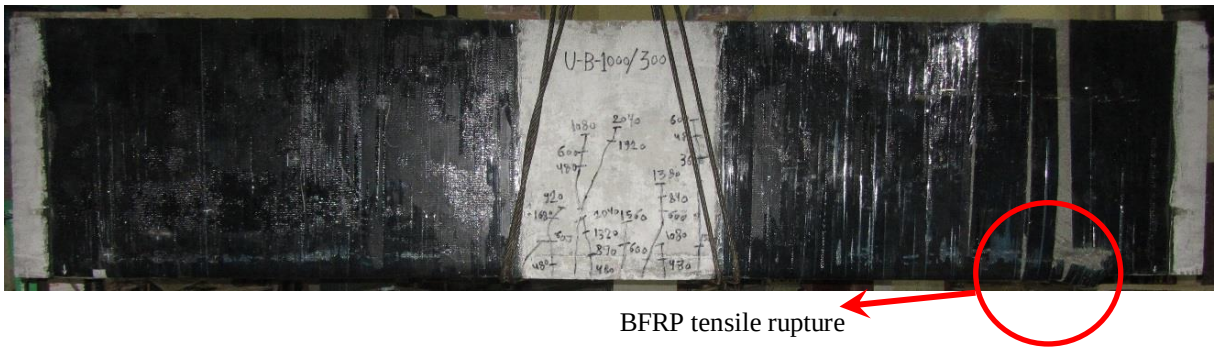

Figure 7. Strengthened beam crack pattern (U-B-1000/300)

3.1.2. Large-scale Beam Series (1000/400)

The first crack in control beam C-1000/400 was observed at the mid-span of the beam at the bottom concrete surface under a cracking load of 440 kN. Increasing the applied load caused the crack to increase and the first crack formed at the shear zone under a cracking load of 620 kN. The final mode of failure was noted to be a shear-type failure with an angle of inclination of 36° to the horizontal axis, as shown in Figure 8. The ultimate load capacity of C-1000/400 was 1600 kN.

The first crack in beam U-B-1000/400 strengthened with four layers of BFRP sheet U-jacketing, started at the bottom concrete surface in the flexural zone under a load application point at a cracking load of 540 kN, and propagated vertically up to two-thirds of the height of the beam, as shown in Figure 9. The ultimate load capacity was 3050 kN, 1.91 times greater than that of the control beam C-1000/400. The mode of failure was noted to be a BFRP debonding failure, as shown in Figure 9.

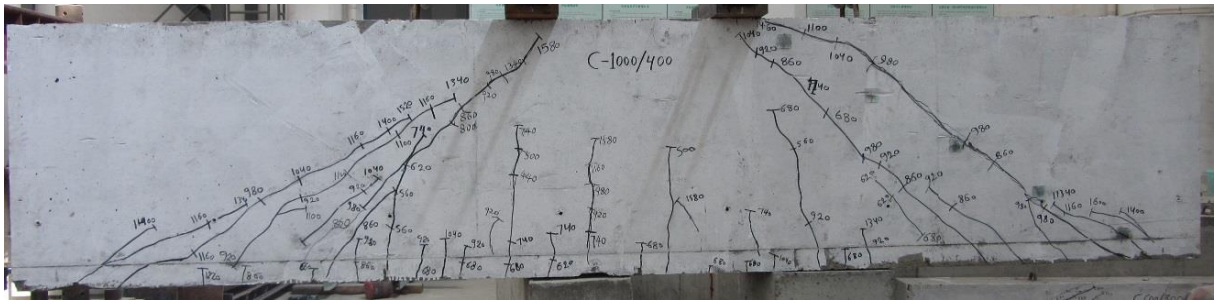

Figure 8. Control beam crack pattern (C-1000/400)

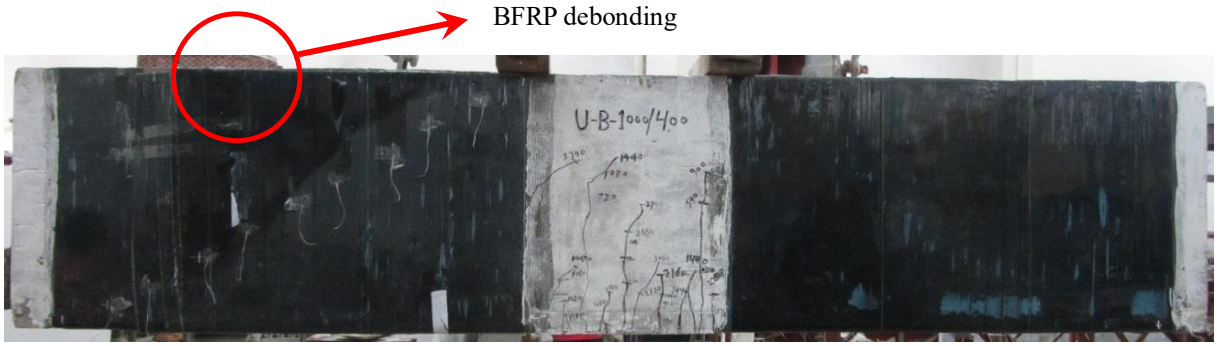

Figure 9. Strengthened beam crack pattern (U-B-1000/400)

3.1.3. Large-scale Beam Series (1000/500)

The first crack in control beam C-1000/500 was observed at the mid-span of the beam at the bottom concrete surface under a cracking load of 630 kN. Increasing the applied load caused the crack to increase and the first crack was observed at the shear zone under a cracking load of 810 kN. The final mode of failure was noted as being shear-type with an angle of inclination of 30° to the horizontal axis, as shown in Figure 10. The beam test specimen failed at an applied ultimate load of 1950 kN.

The first crack in beam U-B-1000/500, strengthened with four layers of BFRP sheet U-jacketing, started at the bottom concrete surface in the flexural zone at the mid-span under a cracking load of 720 kN and propagated vertically up to two-thirds of the height of the beam, as shown in Figure 11. The ultimate load was 3860 kN, 1.98 times greater than that of control beam C-1000/500. The mode of failure was noted as being BFRP tensile rupture failure, as shown in Figure 11.

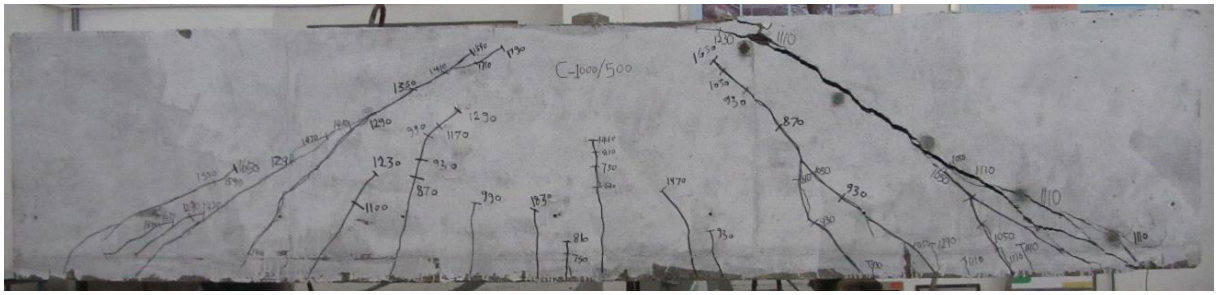

Figure 10. Control beam crack pattern (C-1000/500)

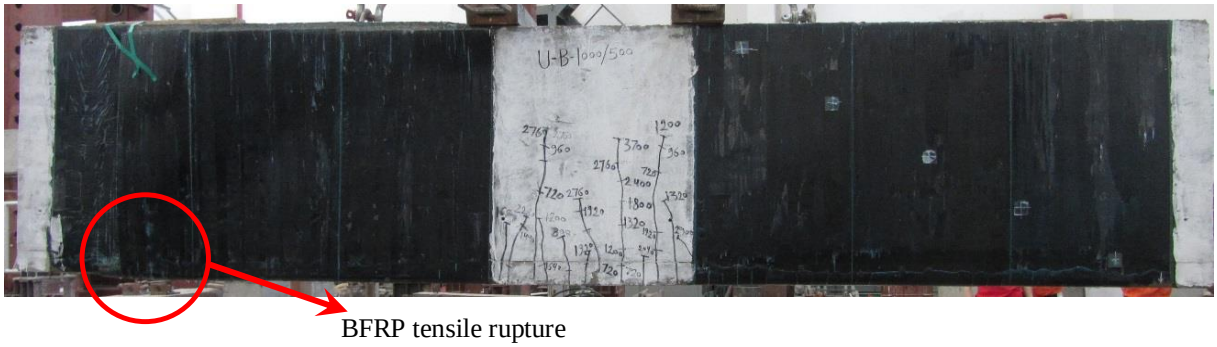

Figure 11. Strengthened beam crack pattern (U-B-1000/500)

It was observed that the angle of crack failure in the control beam changed depending on the ratio between its depth and width. It was found that by decreasing the ratio, the angle decreased in the order: 43°, 36°, and 30°, for depth to width ratios of 3.33, 2.50, and 2.00, respectively. Table 2 shows the cracking and ultimate shear load capacities for the control and strengthened beams along with the ratio between them and the failure modes for the different beam series.

Table 2. Summarized experimental test results for the present study

Beam specimen	*b* (mm)	*h* (mm)	Experimental test results				
			Cracking load (kN)	% Increases	Ultimate load (kN)	% Increases	Failure mode
C-1000/300	300	1000	300	---	1260	---	S
C-1000/400	400	1000	440	---	1600	---	S
C-1000/500	500	1000	630	---	1950	---	S
U-B-1000/300	300	1000	360	20.00%	2440	93.65%	TR
U-B-1000/400	400	1000	540	22.70%	3050	90.63%	BF
U-B-1000/500	500	1000	720	14.29%	3860	97.95%	TR

S= shear failure, BF = debonding failure, and TR = tensile rupture failure.

3.2. Load–Deflection Relationships

At the point of maximum deflection, the measured values at the bottom surface were plotted against the applied load from zero loads up to the point of failure for all tested beams. All measured and plotted values indicated that the deflection increased as the applied load increased. The relationship between the applied load and corresponding maximum deflection was approximately linear at the beginning of the relationship up to a point near to the cracking load, and was predominantly non-linear at higher loads, as shown in Figures 12 to 14. The slope of the linear relationship was predominantly dependent upon the various parameters included in this study.

It is a well-known fact that the deflection under any load level for a strengthened beam is typically smaller than that of a control beam under the same load. However, the maximum measured loads and deflections at failure for strengthened beams are typically bigger than those of control beams.

From the figures, it can be seen that the plots showing the relationship between load and deflection do not indicate a yielding stage because the observed failure mode was a shear failure; whereas for the control beams, the curve showed a smooth deflection. This is the reason for the occurrence of the sudden failure in strengthened beams.

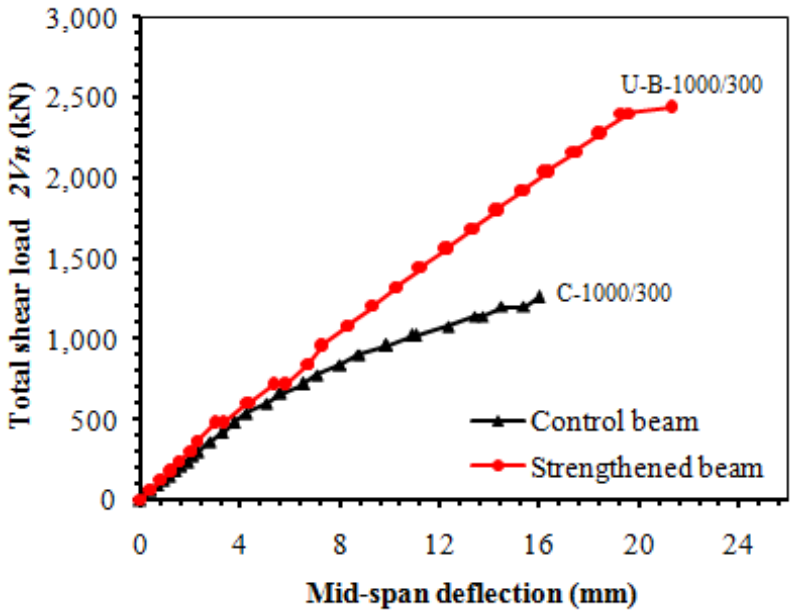

Figure 12. Load deflection curves for strengthened and control beams from beam series (1000/300)

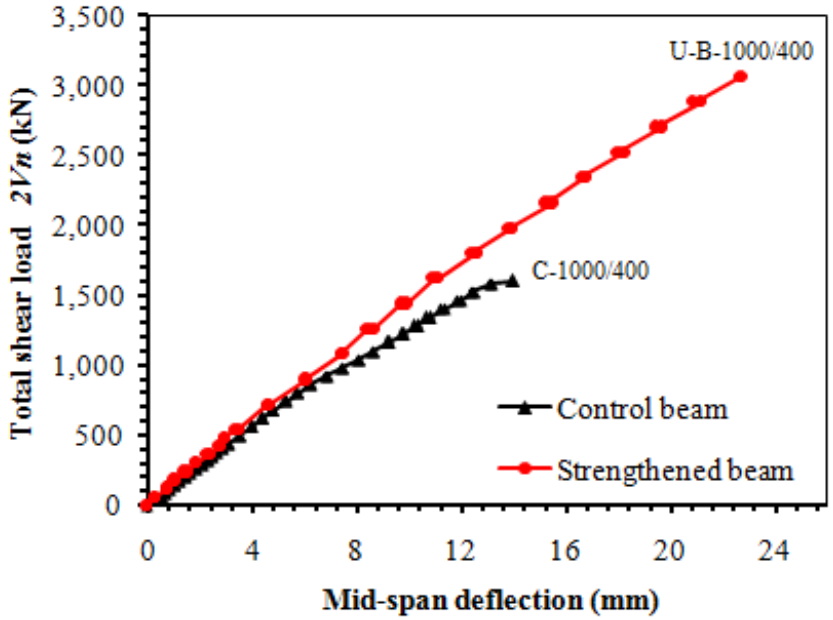

Figure 13. Load deflection curves for strengthened and control beams from beam series (1000/400)

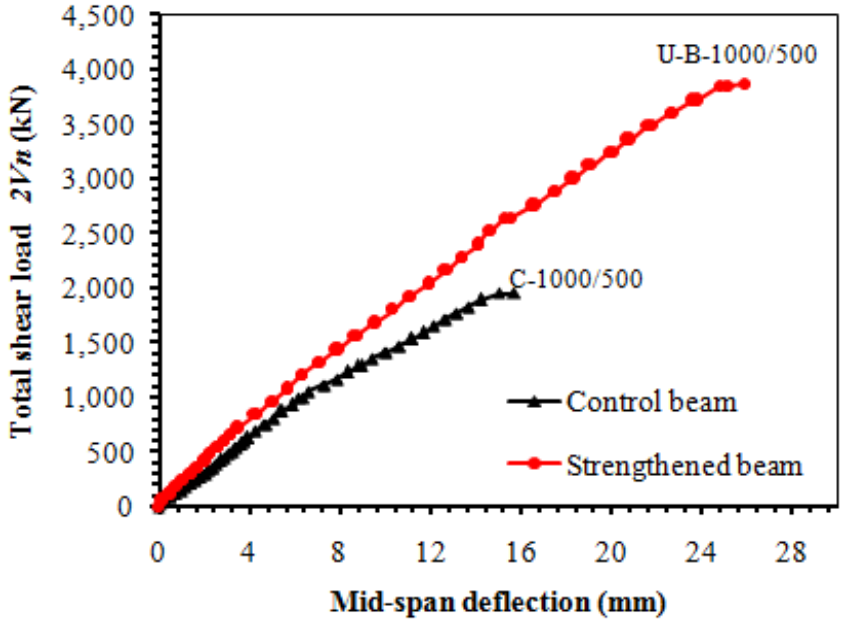

Figure 14. Load deflection curves for strengthened and control beams from beam series (1000/500)

3.3. Maximum Deflection

Figures 12 to 14 clearly show that for all beams and beam widths, increasing the applied load will typically increase the maximum deflection. The rate of increase was mainly dependent on the beam width and the shear zone strengthening, an increase in either of which caused a reduction in the rate of increase. This decrease can be seen in the cracking load at maximum deflection, which was measured at mid-span as shown in Figure 15. From the figure, it can be seen that by increasing the width of the beams, the deflection at the cracking load decreased. However, the ultimate measured value of the deflection at the point of failure for the strengthened beams was larger than that of the control beams, as shown in Figure 16. This could be ascribed to an increase in the stiffness of the beams due to the increase in the width of the beam and to shear zone strengthening. Also, the presence of strengthening by BFRP sheets increases the ductility of the RC beams. This is evident from the ultimate deflection for the strengthened RC beams when compared to without strengthened.

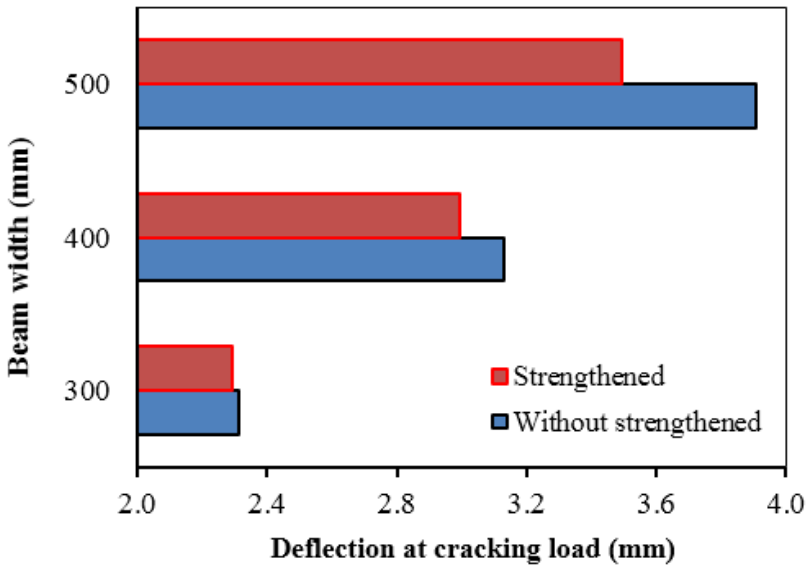

Figure 15. Influence of the beam width on a deflection at the cracking load for the control and strengthened beams

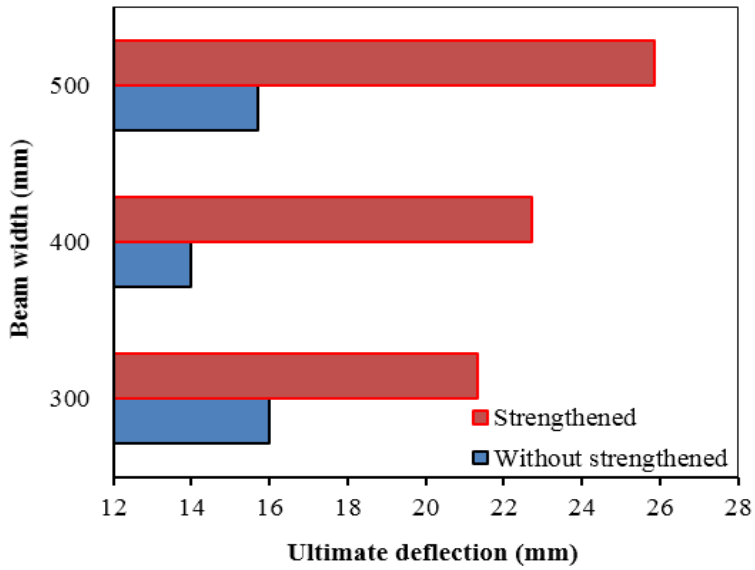

Figure 16. Influence of the beam width on an ultimate deflection for the control and strengthened beams

3.4. Relationship between the Load and Concrete Strain

The concrete strain was measured at the top surface mid-span point and the measured values were plotted against the applied load from zero loads up to failure for the various tested beams. The relationship between the applied shear force and the concrete strain for all beams is shown in Figure 17.

For beam series 1000/300, the rate of decrease was considered high for the strengthened beam under any load when compared to the control beam. Additionally, the measured maximum concrete strain at failure load for the strengthened beam U-B-1000/300 was found to be nearly identical to that of the control beam C-1000/300.

The characteristics of the relationship between load and concrete strain for all large-scale beam series (1000/400 and 1000/500) were similar to those of beam series 1000/300, as shown in Figure 17. For all beam series, it was clear that the effect of beam width and the bonded sheet strengthening on concrete compression strain was typically nearly identical to their effect on the deflection relationship. Additionally, the measured maximum mid-span concrete strain at failure load for the strengthened beams was considered low it was thus deduced that no crushing will occur at the concrete compression zone at the top surface of the beams.

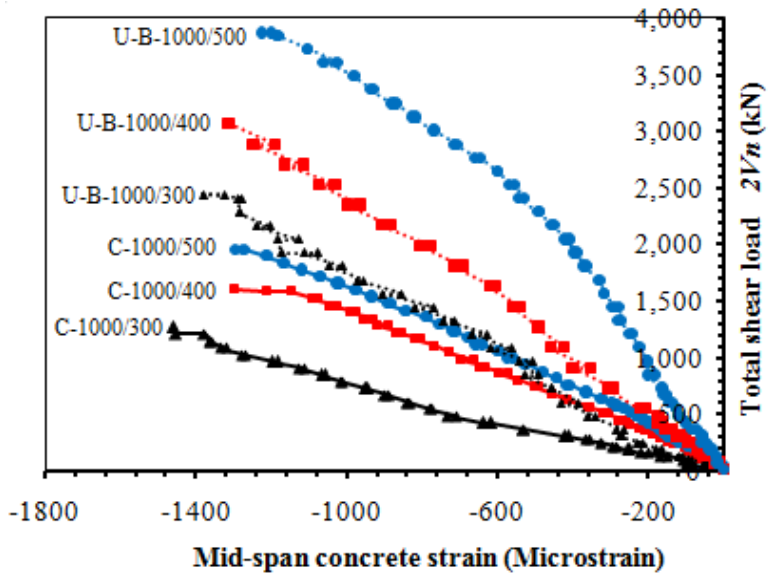

Figure 17. Plots of load with respect to concrete strain in the compression face for control and strengthened beams from all beam series

3.5. Out-of-Plane Displacement (Lateral Displacement)

Out-of-plane displacements along the diagonal strut were measured for all beam specimens and plotted as shown in Figures 18 to 20. The beam specimens were tested without load eccentricity. In order to ignore the eccentricity, an average value was taken for both sides at every point.

From these figures, it can be observed that the value of the out-of-plane displacements of the strengthened beams was smaller than those of the control beams under the same load, such as the failure load for the control beam. This deficiency in out-of-plane displacements is caused by the presence of U-jacketing strengthening by BFRP sheets. However, the ultimate value of the out-of-plane displacements for the strengthened beams was larger than that of the control beams at the failure load. This was deemed to be due to the sides not being added with BFRP sheets. The horizontal part of the BFRP sheets was thus unable to control lateral movement in the beam.

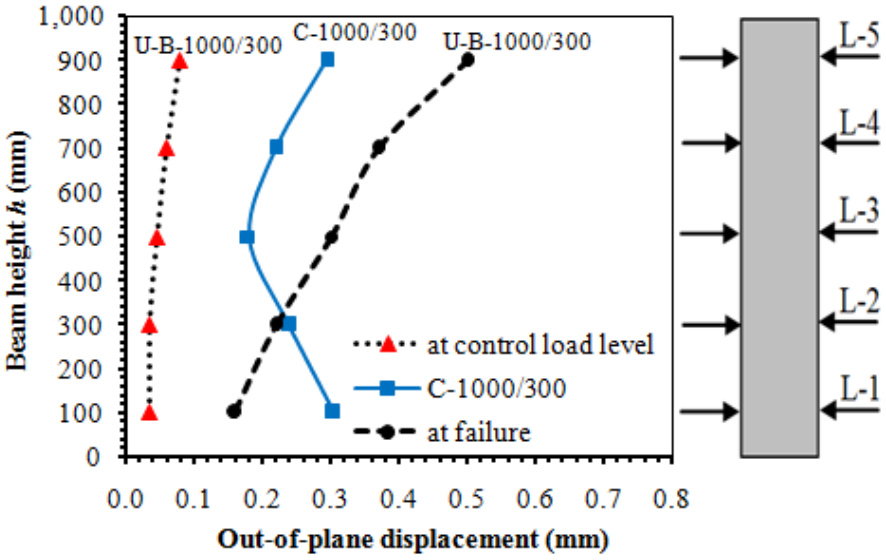

Figure 18. Out-of-plane displacement at the failure load for specimens C-1000/300 and U-B-1000/300

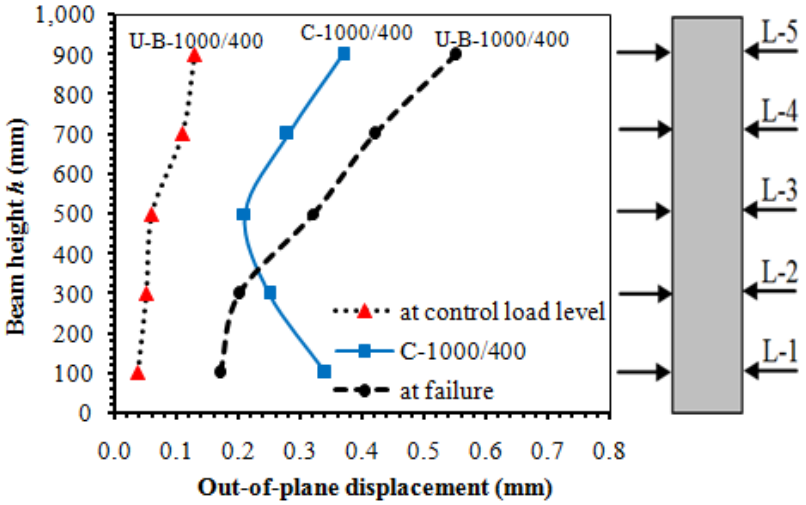

Figure 19. Out-of-plane displacement at the failure load for specimens C-1000/400 and U-B-1000/400

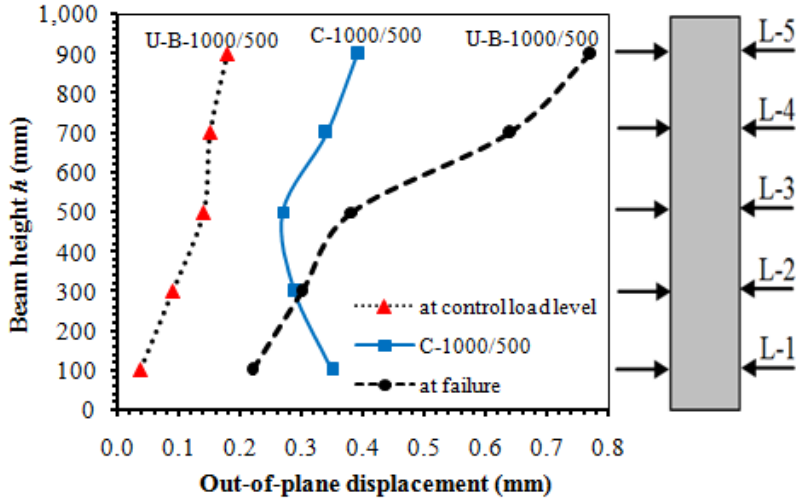

Figure 20. Out-of-plane displacement at the failure load for specimens C-1000/500 and U-B-1000/500

For beams strengthened with U-jacketing confinement, debonding failure can occur at the top surface of the beam, as shown in Figure 21. For the bottom surface of the beam, since out-of-plane displacements are controlled by the horizontal part of the BFRP sheets, no debonding will occur. This allows the value of the shear load capacity to be increased up to the tensile rupture failure capacity of the BFRP sheets, as shown in Figure 22.

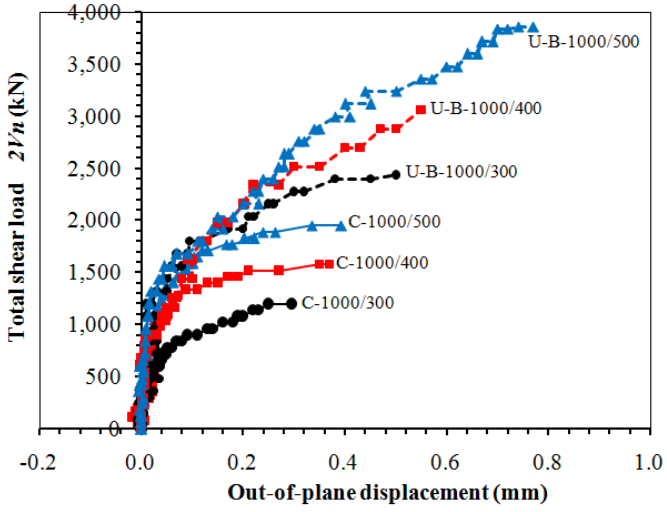

Figure 21. Load with respect to out-of-plane displacement at point (5) at the top surface of beams

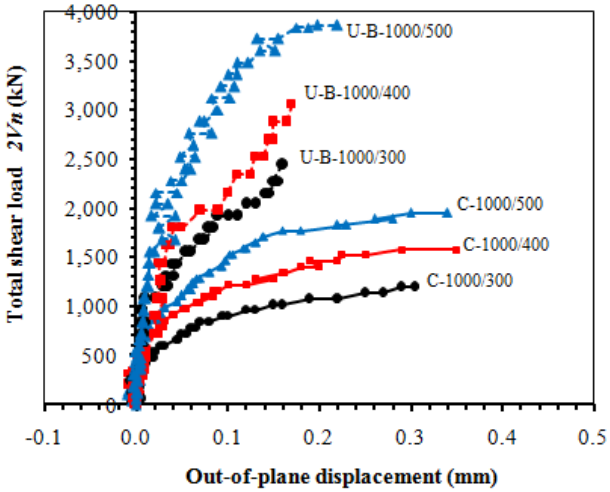

Figure 22. Load with respect to out-of-plane displacement at point (1) at the bottom surface of beams

3.6. Influence of the Beam Width

The width of the beam had a significant, direct influence on the out-of-plane displacement, as shown in Figure 23, as well as on the lateral strain, as shown in Figure 24. This lateral strain on the edges of the beam can be controlled by the horizontal part of the FRP sheets by using U-jacketing strengthening or completely wrapped. The relationship between the beam height and lateral concrete strain for different beam widths at failure is shown in Figure 24. When the width of the beam increased, the lateral strain decreased, which led to slow debonding failure or a change to fiber rupture failure.

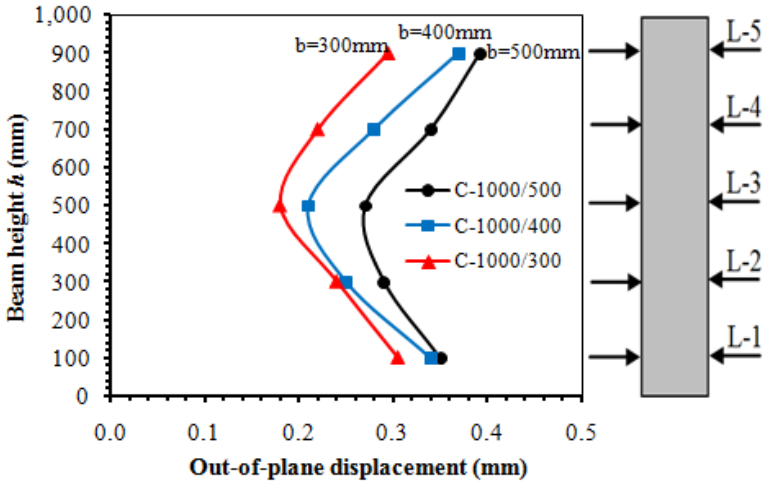

Figure 23. Relationship between beam height and out-of-plane displacement for different beam widths at failure

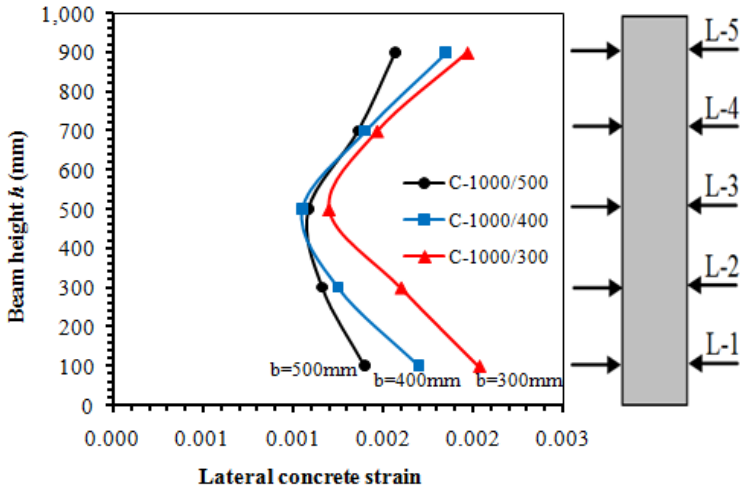

Figure 24. Relationship between beam height and lateral concrete strain for different beam widths at failure

3.7. Effective Strain on BFRP Sheets

The strains in the fiber direction of the vertical BFRP sheet were measured using 9 strain gages positioned in the test region, as shown in Figure 25. The results were plotted at the failure load levels (25%, 50%, 75%, and 100% of ultimate load), as shown in Figures 26 to 28. From these figures, it can be seen that in the case of tensile rupture failure, the BFRP sheet strain distribution can be seen to be spread across all locations for any load level. This implied that the BFRP sheet was very efficient at distributing strain. The BFRP sheet strain distribution effect did not have to create an even distribution at every location in the case of debonding failure and therefore fell behind tensile rupture failure in terms of efficiency. This implied that the strain was concentrated in one location, so debonding failure was bound to happen earlier than tensile rupture. Therefore, if the FRP sheets as a completely wrapped strengthened are used around the cross-section, then the occurrence of the tensile rupture of the FRP, as a result, happens and thus it can obtain the maximum efficiency of the FRP material.

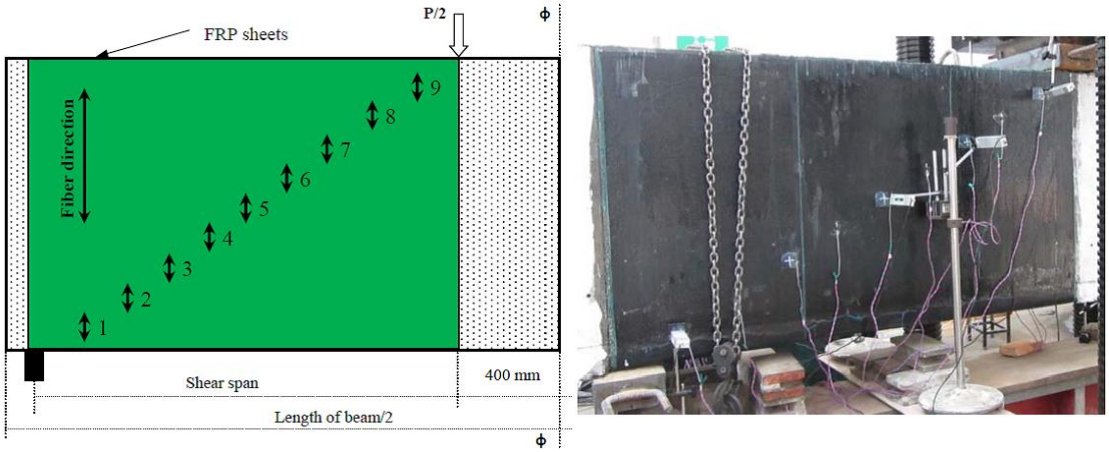

Figure 25. Typical number, location, and direction of strain gauges mounted on the BFRP sheet for the strengthened beams

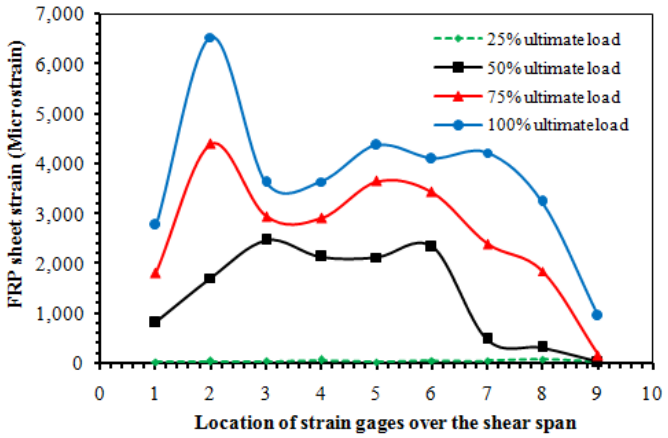

Figure 26. Vertical BFRP sheet strain distribution over the shear span for strengthened beam U-B-1000/300

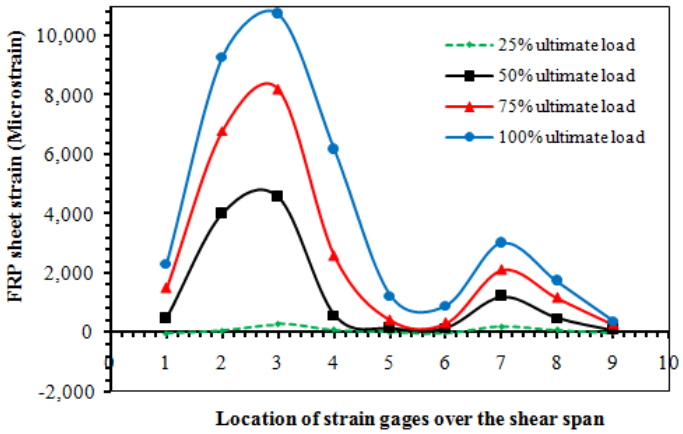

Figure 27. Vertical BFRP sheet strain distribution over the shear span for strengthened beam U-B-1000/400

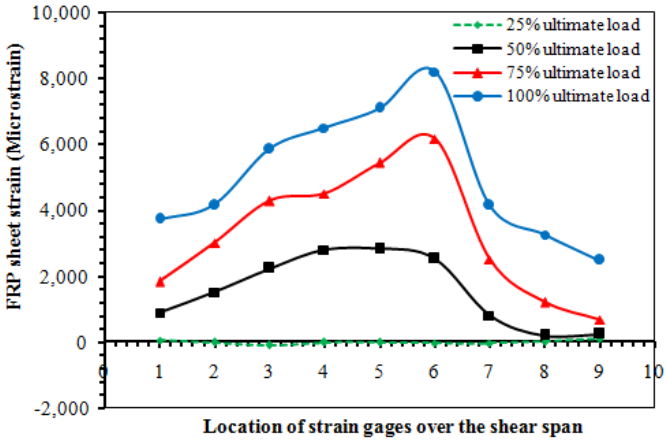

Figure 28. Vertical BFRP sheet strain distribution over the shear span for strengthened beam U-B-1000/500

4. Conclusions

Based on the experimental test results conducted on large-scale RC beams strengthened with BFRP sheets, it was evident that the BFRP sheets provided appreciable enhancement and increased both the toughness and ultimate strength of the strengthened beams in comparison to the control beams.

- For beams with widths of 300, 400, and 500mm, it was observed that by using BFRP sheets for strengthening, both the cracking and ultimate load increased in comparison to the control beams under the same conditions. The cracking load of the 300, 400, and 500mm wide strengthened beams was 1.20, 1.23, and 1.14 times greater than that of the control beams, respectively. Additionally, the ultimate load of the 300, 400, and 500 mm wide strengthened beams was 1.94, 1.91, and 1.98 times greater than that of the control beams, respectively.
- Varying the depth to width ratio of the beam caused variation in the failure angle as well. By increasing this ratio, the angle of failure likewise increased. Ratios of 2.00, 2.50, and 3.33 yielded failure angles of 30^{o}, 36^{o}, and 43^{o}, respectively.
- Variations in beam width caused variations in the lateral strain as well, in an inversely proportional relationship.
- The BFRP sheet strain was very well distributed in the case of tensile rupture, but this was not so in the case of debonding failure where the BFRP sheet strain was concentrated at a specific location.

5. Acknowledgements

The deanship of Scientific Research, Majmaah University, deserves special thanks for his generous support in the accomplishment of this task under Project Number No. 1439-46.

6. Conflicts of Interest

The authors declare no conflict of interest.

7. References

[1] ACI Committee 440. “Guide for the Design and Construction of Externally Bonded FRP Systems for Strengthening Concrete Structures.” (ACI 440.2R-17). American Concrete Institute, Farmington Hills, Michigan, USA. (2017).

[2] Triantafillou, Thanasis C., and Costas P. Antonopoulos. “Design of Concrete Flexural Members Strengthened in Shear with FRP.” Journal of Composites for Construction 4, no. 4 (November 2000): 198–205. doi:10.1061/(asce)1090-0268(2000)4:4(198).

[3] Matthys, Stijn, and Thanasis Triantafillou. “Shear and Torsion Strengthening with Externally Bonded FRP Reinforcement.” Composites in Construction (December 18, 2001): 203-212. doi:10.1061/40596(264)22.

[4] Mofidi, Amir, and Omar Chaallal. "Shear strengthening of RC beams with EB FRP: Influencing factors and conceptual debonding model." Journal of Composites for Construction 15, no. 1 (2011): 62-74. doi:10.1061/(ASCE)CC.1943-5614.0000153.

[5] Ye L.P., Lu X.Z., and Chen J.F. “Design Proposals for Debonding Strengths of FRP Strengthened RC Beams in the Chinese Design Code.” Proc., Int. Symp. on Bond Behaviour of FRP in Structures, International Institute for FRP in Construction (IIFC), Hong Kong, China, December (2005): 55-62.

[6] Cao, S. Y., J. F. Chen, J. G. Teng, Z. Hao, and J. Chen. "Debonding in RC beams shear strengthened with complete FRP wraps." Journal of Composites for Construction 9, no. 5 (2005): 417-428. doi:10.1061/(ASCE)1090-0268(2005)9:5(417).

[7] Carolin, Anders, and Björn Täljsten. "Theoretical study of strengthening for increased shear bearing capacity." Journal of Composites for Construction 9, no. 6 (2005): 497-506. doi:10.1061/(ASCE)1090-0268(2005)9:6(497).

[8] Colotti, Vincenzo, Giuseppe Spadea, and R. Narayan Swamy. "Analytical model to evaluate failure behavior of plated reinforced concrete beams strengthened for shear." Structural Journal 101, no. 6 (2004): 755-764.

[9] Sayed, Ahmed M., Xin Wang, and Zhishen Wu. "Modeling of shear capacity of RC beams strengthened with FRP sheets based on FE simulation." Journal of Composites for Construction 17, no. 5 (2013): 687-701. doi:10.1061/(ASCE)CC.1943-5614.0000382.

[10] Adhikary, Bimal Babu, and Hiroshi Mutsuyoshi. "Behavior of concrete beams strengthened in shear with carbon-fiber sheets." Journal of composites for construction 8, no. 3 (2004): 258-264. doi:10.1061/(ASCE)1090-0268(2004)8:3(258).

[11] Zhang, Zhichao, and Cheng-Tzu Thomas Hsu. "Shear strengthening of reinforced concrete beams using carbon-fiber-reinforced polymer laminates." Journal of composites for construction 9, no. 2 (2005): 158-169. doi:10.1061/(ASCE)1090-0268(2005)9:2(158).

[12] Spinella, Nino. "Modeling of shear behavior of reinforced concrete beams strengthened with FRP." Composite Structures 215 (2019): 351-364. doi:10.1016/j.compstruct.2019.02.073.

[13] Issa, Mohsen A., Thilan Ovitigala, and Mustapha Ibrahim. "Shear Behavior of Basalt Fiber Reinforced Concrete Beams with and Without Basalt FRP Stirrups." Journal of Composites for Construction 20, no. 4 (August 2016): 04015083. doi:10.1061/(asce)cc.1943-5614.0000638.

[14] Shen, Dejian, Xuan Zeng, Jinyang Zhang, Baizhong Zhou, and and Wei Wang. "Behavior of RC box beam strengthened with basalt FRP using end anchorage with grooving." Journal of Composite Materials 53, no. 23 (2019): 3307-3324. doi:10.1177/0021998319826376.

[15] Guo, Rui, Lianheng Cai, Shinichi Hino, and Bo Wang. "Experimental Study on Shear Strengthening of RC Beams with an FRP Grid-PCM Reinforcement Layer." Applied Sciences 9, no. 15 (2019): 2984. doi:10.3390/app9152984.

[16] Atutis, Mantas, Juozas Valivonis, and Edgaras Atutis. "Experimental Study of Concrete Beams Prestressed with Basalt Fiber Reinforced Polymers. Part I: Flexural Behavior and Serviceability." Composite Structures 183 (January 2018): 114–123. doi:10.1016/j.compstruct.2017.01.081.

[17] Kadhim, Asaad M. H., Hesham A. Numan, and Mustafa Özakça. "Flexural Strengthening and Rehabilitation of Reinforced Concrete Beam Using BFRP Composites: Finite Element Approach." Advances in Civil Engineering 2019 (March 4, 2019): 1–17. doi:10.1155/2019/4981750.

[18] Joyklad, Panuwat, Suniti Suparp, and Qudeer Hussain. "Flexural Response of JFRP and BFRP Strengthened RC Beams." International Journal of Engineering and Technology (November 3, 2019): 203–207. doi:10.7763/ijet.2019.v11.1147.

[19] Colajanni, Piero, Lidia La Mendola, Antonino Recupero, and Nino Spinella. "Stress Field Model for Strengthening of Shear-Flexure Critical RC Beams." Journal of Composites for Construction 21, no. 5 (October 2017): 04017039. doi:10.1061/(asce)cc.1943-5614.0000821.

[20] Wu, Qiaoyun, Shiye Xiao, and Kentaro Iwashita. "Experimental Study on the Interfacial Shear Stress of RC Beams Strengthened with Prestressed BFRP Rod." Results in Physics 10 (September 2018): 427–433. doi:10.1016/j.rinp.2018.06.007.

[21] Pellegrino, Carlo, and Claudio Modena. "Fiber reinforced polymer shear strengthening of reinforced concrete beams with transverse steel reinforcement." Journal of Composites for Construction 6, no. 2 (2002): 104-111. doi:10.1061/(ASCE)1090-0268(2002)6:2(104).

[22] Sayed, Ahmed M., Xin Wang, and Zhishen Wu. "Finite Element Modeling of the Shear Capacity of RC Beams Strengthened with FRP Sheets by Considering Different Failure Modes." Construction and Building Materials 59 (May 2014): 169–179. doi:10.1016/j.conbuildmat.2014.02.044.

[23] Deniaud, Christophe, and JJ Roger Cheng. "Review of Shear Design Methods for Reinforced Concrete Beams Strengthened with Fibre Reinforced Polymer Sheets." Canadian Journal of Civil Engineering 28, no. 2 (April 1, 2001): 271–281. doi:10.1139/l00-113.

[24] Ahmed, Ehab A., Ehab F. El-Salakawy, and Brahim Benmokrane. "Shear Performance of RC Bridge Girders Reinforced with Carbon FRP Stirrups." Journal of Bridge Engineering 15, no. 1 (January 2010): 44–54. doi:10.1061/(asce)be.1943-5592.0000035.

[25] Belarbi A., Murphy M., and Bae S.W. "Shear Strengthening of Full-Scale RC T-Beams with CFRP Sheets." APFIS 2012, Hokkaido University, Japan, (2-4 February 2012), S1A02.

[26] Godat, Ahmed, and Omar Chaallal. "Strut-and-Tie Method for Externally Bonded FRP Shear-Strengthened Large-Scale RC Beams." Composite Structures 99 (May 2013): 327–338. doi:10.1016/j.compstruct.2012.11.034.

[27] Matta F., Nanni A., Galati N., and Mosele F. "Size Effect on Shear Strength of Concrete Beams Reinforced with FRP Bars." Proc. 6th Int. Conf. on Fracture Mechanics of Concrete and Concrete Structures (FraMCoS-6), Catania, Italy, (June 17-22, 2007): 8 pp.